Article

Singlet oxygen photooxidation of peptidic oxazoles and thiazoles

Alessandro Manfrin, Nadine Borduas-Dedekind, Kate Lau, and Kristopher McNeill

J. Org. Chem., **Just Accepted Manuscript** • DOI: 10.1021/acs.joc.8b02684 • Publication Date (Web): 25 Jan 2019

Singlet oxygen photooxidation of peptidic oxazoles and thiazoles

Alessandro Manfrin, Nadine Borduas-Dedekind, Kate Lau, Kristopher McNeill*

Institute of Biogeochemistry and Pollutant Dynamics, Department of Environmental Systems Science, ETH Zurich, 8092 Zurich, Switzerland

ABSTRACT: Oxazoles and thiazoles are commonly found moieties in nonribosomal peptides (NRPs) and ribosomally synthesized post-translationally modified peptides (RiPPs), which are important biomolecules present in the environment and in natural waters. From previous studies, they seem susceptible to oxidation by singlet oxygen ($^1O_2$), therefore we designed and synthesized model oxazole- and thiazole-peptides and measured their $^1O_2$ bimolecular reaction rate constants, showing slow photooxidation under environmental conditions. We reasoned their stability through the electron-withdrawing effect of the carboxamide substituent. Reaction products were elucidated and support a reaction mechanism involving cycloaddition followed by a series of rearrangements. The first $^1O_2$ bimolecular reaction rate constant for a RiPP, the thiazole-containing peptide Aerucyclamide A, was measured and found in good agreement with the model peptide's rate constant, highlighting the potential of using model peptides to study the transformations of other environmentally relevant NRPs and RiPPs.

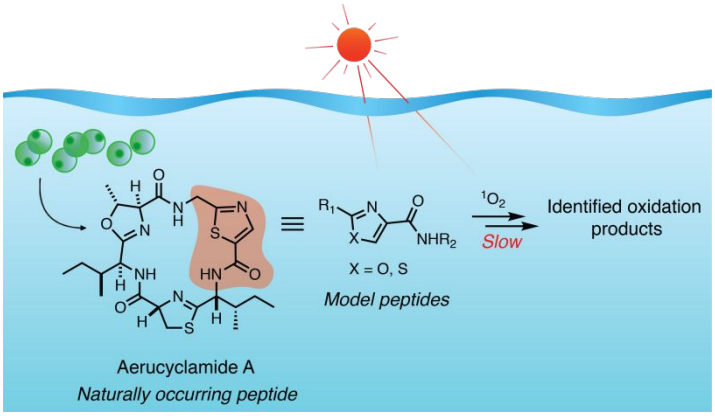

Introduction

Amino acid-based oxazoles and thiazoles are formed from the cyclization of serine, threonine, and cysteine side chains onto the peptide backbone and are common features of nonribosomal peptides (NRPs) and ribosomally encoded post-translationally modified peptides (RiPPs).[1,2] We are particularly interested in NRP and RiPP natural products since they have the potential to act as water contaminants and as ecologically important biomolecules (e.g., metal-binding siderophores). Such oxazole and thiazole peptides have been isolated from sunlight-dwelling photosynthetic algae, cyanobacteria, sea slugs and sponges.[2,3–11] However, the prevalence of these peptidic heterocycles would seem counterintuitive if they are as reactive toward singlet oxygen ($^1O_2$), a ubiquitous oxidant in sunlit natural waters, as previously studied oxazoles and thiazoles.[12–15] Indeed, earlier work by Nakamura et al. and by Wasserman et al. showed that phenyl-substituted oxazoles react quickly with $^1O_2$ with rate constants on the order of 10^7 - 10^8 $M^{-1}s^{-1}$, translating to a half-life of only 4 days for the highest rate constant in the presence of a typical fresh water $^1O_2$ concentration of 1.4×10^{-14} M (Scheme 1).[16,17] Beside that, such peptides could be degraded also by intracellular $^1O_2$, that is well known to be present in both photosynthetic and non-photosynthetic cells.[18] This relatively high reactivity toward $^1O_2$ suggests that oxazole-containing NRPs and RiPPs could be susceptible to photooxidation, limiting their environmental lifetime and thus their potential for contamination, but simultaneously questioning their biosynthetic utility.

As for thiazole-containing peptides, they are also potential targets for oxidation by $^1O_2$. In fact, thiazoles have been shown to react with $^1O_2$ in an analogous manner as oxazoles, yielding similar triamide products.[19] Currently, rate constants for the reaction of thiazoles with $^1O_2$ are essentially absent from the literature. Moreover, there is currently no information on the photoreactivity of oxazole and thiazoles with the relevant substitution pattern found in NRP and RiPP natural products. Oxazoles and thiazoles moieties are not only found in natural products, but are also common in drug design,[20] including Dasatinib, a chemotherapeutic blockbuster drug which contains a peptidic thiazole motif.[21] We therefore sought to evaluate the fate of oxazoles and thiazoles in environmentally relevant peptides to better understand their fate in natural waters. Given the previous work on $^1O_2$ reactivity of oxazoles and thiazoles, we focused on this oxidant, being aware of the fact that $^1O_2$ is only one member of a larger group of reactive species.

Here, we examine a series of model peptides, designed to assess the reactivity of natural NRPs and RiPPs containing oxazole and thiazole rings. We report the synthesis of these amino acid-based oxazoles and thiazoles and the examination of their photoreactivity with an emphasis on their reactivity

toward $^1O_2$. In addition, we report the $^1O_2$ reactivity of the cyanobacterial natural product, Aerucyclamide A, in relation to that predicted by our model peptide series. Finally, we propose a mechanism consistent with our computational chemistry results and with the product distribution for the $^1O_2$ reaction with oxazole and thiazole peptides.

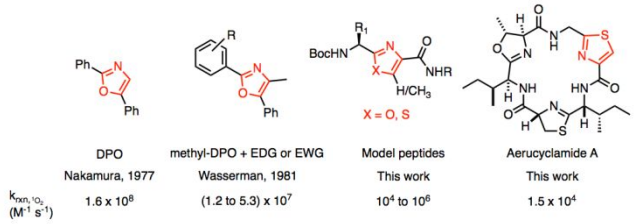

Scheme 1. $^1O_2$ rate constants for oxazoles and thiazoles from prior studies and the present contribution.

Results

Synthesis of model peptides

Three different oxazole- and thiazole-derivatives of the amino acid L-valine were chosen as representative peptides to study the photochemistry of oxazole- and thiazole-containing natural products (Scheme 2). We chose L-valine because it is often involved in ring closure reactions to form oxazole or thiazole moieties in natural peptides.[22–31] Two additional model oxazole-peptides were synthesized from glycine and L-phenylalanine, to assess the influence of the neighboring side chain on their reactivity.

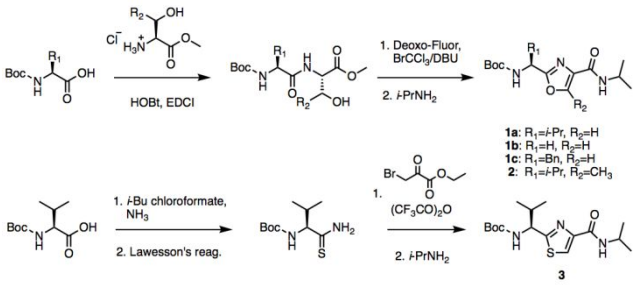

Scheme 2. Synthesis of oxazole- and thiazole-containing peptides.

Oxazole model peptides were prepared in three steps from the Boc-protected amino acids and L-serine or L-threonine methyl ester hydrochloride by a coupling reaction.[32] The dipeptide was treated first with Deoxo-Fluor reagent and $BrCCl_3$/DBU,[33] and then with isopropyl amine to give the desired model oxazole peptides (Scheme 2) **1a**, **1b**, **1c** and **2** in 18%, 17%, 24% and 42% yields, respectively. The thiazole variant required the use of Boc-L-valine-NH_2, synthesized from Boc-L-valine-OH using isobutyl chloroformate and aqueous ammonia solution,[34] and then converted in the thioamide by treatment with Lawesson's reagent (Scheme 2). The desired model thiazole peptide was obtained in two steps from this thioamide by reaction with ethyl bromopyruvate and acetic anhydride,[35] followed by treatment with isopropyl amine (Scheme 2) in 22% overall yield.

$^1O_2$ bimolecular rate constant determination

The direct photoreactivity of model peptides **1a**, **2** and **3** was studied in a photoreactor by exposing the test molecules to UVA and UVB light. These experiments demonstrate complete photostability of the peptides over a period of 8 hours, indicating that no significant direct photodegradation can be expected under natural sunlight conditions (see SI Figure S28). Peptides **1a**, **2**, and **3** were then exposed to sensitized photolysis using perinaphthenone as a $^1O_2$ sensitizer. The choice of perinaphthenone as $^1O_2$ sensitizer was due to its high photostability and $^1O_2$ quantum yield and low excited state reduction potential under UVA irradiation.[36,37] Surprisingly, in comparison to the previously reported phenyl-oxazoles, the model peptides showed slow reactivity towards $^1O_2$.

The rate constants we obtained are summarized in Table 1. The oxazole-containing peptide **1a** showed a rate constant of 2.0×10^5 $M^{-1}s^{-1}$, which is 14 times larger than for the thiazole peptide **3**, the slowest in the series. The fastest reacting peptide was the methoxazole peptide **2**, degrading with a rate constant of 1.27×10^6 $M^{-1}s^{-1}$. These rate constants are notably low compared to the previously reported rate constant for diphenyloxazole (DPO) on the order of 10^8 $M^{-1}s^{-1}$.[5] This gap in reactivity of 2 to 3 orders of magnitude prompted us to re-assess the $^1O_2$ rate constant for DPO with our experimental setup. We determined it to be $(1.0 \pm 0.3) \times 10^7$ $M^{-1}s^{-1}$, one order of magnitude smaller than previously reported (Table 1). Of note, we believe that the previous value of $^1O_2$ reaction rate constant may be overestimated due to the contribution of $^1O_2$ physical quenching to the measurement, since the $^1O_2$ rate constant was obtained using a laser-based phosphorescence quenching technique that cannot distinguish between physical and chemical quenching.[16] In this work, the measurements were conducted using a steady-state approach, free from $^1O_2$ physical quenching contributions. Despite this, a large reactivity gap between DPO and our peptide-based oxazoles remained, which led to the question of why the amino acid-based oxazoles and thiazoles show such poor reactivity towards $^1O_2$. Having in mind that $^1O_2$ prefers to react with electron-rich rings,[38] we reasoned that the carboxamide functional group deactivates the ring towards this reaction.

To explore this structure-activity relationship, we prepared a set of oxazole and thiazole derivatives that allowed us to isolate the effect of an electron-withdrawing substituent on the ring. We compared 2-methyloxazole (**5**) with *N*-isopropyl-2-methyloxazole-4-carboxamide (**6**) and found that the $^1O_2$ bimolecular rate constant was 6 times higher for the non-carboxamide-containing oxazole (Fig. 1, A). A similar, but weaker effect is observed in the thiazole series (compounds **7** and **8**), where the carboxamide cut the reactivity with $^1O_2$ in half (Fig.1, B). We ascribe this effect to the electron-withdrawing character of the substituent, which makes intrinsically electron-poor rings, such as oxazoles and thiazoles,[39] even more electron-deficient. We observed the same effect with furans, which are well-known $^1O2$ acceptors.[40,41] Carboxamide-substitution decreased the reaction rate constant from 9.6 to 3.1 $\times$ 10^8 $M^{-1}s^{-1}$ for 2,5-dimethylfuran, a factor of 3.1 (Table 1).

Furthermore, it is clear that oxazoles are more reactive toward $^1O_2$ than thiazoles (Table 1). Specifically, 2-methyloxazole (**5**) is 57 times more reactive than 2-methylthiazole (**7**), and its carboxamide-substituted analogue (**6**) is 18 times more reactive than the thiazole one (**8**).

Electron donating groups enhance the reactivity of the 5-membered heterocycles towards $^1O_2$ regardless of their position on the ring. Indeed, a C-5 methyl substitution leads to an increase in the $^1O_2$ bimolecular rate constant, with methoxazole peptide **2**, which contains the C-5 methyl, reacting 6 times faster than oxazole peptide **1a**, which does not. This result is consistent with the methyl group increasing the electron density on the C-5, and accelerating the reaction with $^1O_2$.

Prior work has found a variety of amino acids that undergo ring closure reaction with neighboring serine, cysteine or threonine, generating oxazoles and thiazoles with different R groups on the side chain.[7,42] We therefore also investigated the role of steric hindrance with the smallest and the largest possible neighboring groups, originating from glycine and phenylalanine.[43,44] We found that the presence of a smaller group facilitates the reaction with $^1O_2$, while a larger group reduces the reactivity of the ring (Table 1). This difference in the reactivity with $^1O_2$ is ascribed to a weak steric effect of the alkyl neighboring group.

$^1O_2$ bimolecular rate constant of a natural RiPP

To assess the relevance of the model peptide rate constants toward natural NRPs and RiPPs, we measured the bimolecular rate constant for the reaction of $^1O_2$ with Aerucyclamide A (**4**), one of the most abundant cyclic peptides produced by the fresh water cyanobacterium *Microcystis aeruginosa*.[45] The $^1O_2$ bimolecular rate constant of **4** was found to be 1.2×10^4 $M^{-1}s^{-1}$, similar to the rate constant measured for the model thiazole-peptide **3** (1.5×10^4 $M^{-1}s^{-1}$), consistent with the thiazole moiety being the site of reactivity. This result suggests that the model peptides can be used to make first-order predictions of the environmental photochemical fate of naturally occurring NRPs and RiPPs.

Table 1. Experimentally determined $^1O_2$ bimolecular rate constants and calculated vertical ionization potentials (IP) for oxazoles and thiazoles model peptides and comparison compounds.

Entry	Compound	k_{rxn} ($\times 10^4$ $M^{-1}s^{-1}$)	Calculated vertical IP (eV)
1	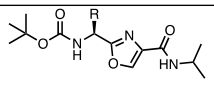		
	1a R = *i*-Pr	20.7 ± 2.0	6.81
	1b R = H	23.7 ± 0.8	6.82
	1c R = CH_2Ph	18.8 ± 0.7	6.80
2	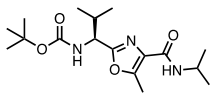	127 ± 4	6.52
3	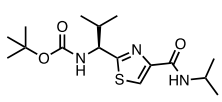	1.5 ± 0.6	6.87
4	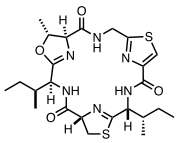	1.2 ± 0.4	n.d.[a]
5		475 ± 9	6.50
6	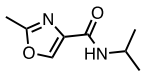	77 ± 9	6.74
7		8.4 ± 0.6	6.62
8	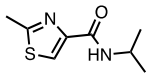	4.2 ± 0.8	6.84
9		96000 ± 500	n.d.[a]
10	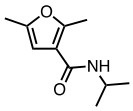	31000 ± 800	n.d.[a]
DPO	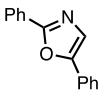	1000 ± 300	n.d.[a]

[a]n.d. = not determined

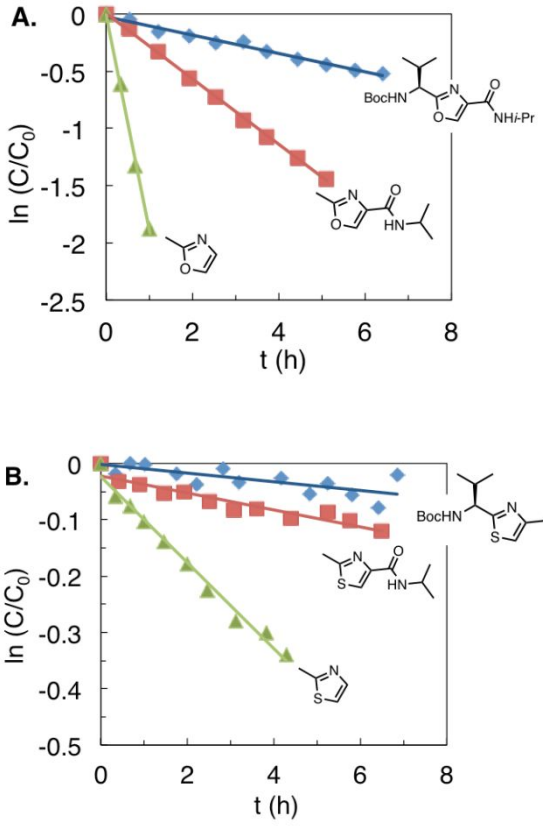

Figure 1. Kinetic traces of oxazoles (A; **1a**, blue diamonds, **5**, green triangles, **6**, red squares) and thiazoles (B; **3**, blue diamonds, **7**, green triangles, **8**, red squares).

Correlation of reactivity with computed electronic energies

To further understand the origin of the stability of oxazoles and thiazoles towards $^1O_2$, DFT calculations were performed. We investigated the effect of the carboxamide group on the electronic character of the heterocyclic aromatic rings. As the rate-determining transition state is believed to involve interaction of $^1O_2$ with the oxazole or thiazole π system, we reasoned that HOMO energies might correlate with $^1O_2$ reactivity. We computed vertical ionization potentials and invoked Koopmans' theorem to correlate them with the HOMO energies of the studied compounds.[46] Others have noted that in Kohn–Sham (KS) DFT calculations, the negative energy of the highest occupied molecular orbital (HOMO) is equivalent to the first ionization potential (vertical IP).[47] We therefore established a structure-activity relationship for the $^1O_2$ rate coefficients with computed vertical ionization energies of a series of oxazoles and thiazoles. A linear free energy relationship (LFER) was found between the computed vertical IPs of oxazoles and thiazoles and $\log_{10} k_{rxn,}{}^{1O2}$ (Fig. 2). The LFERs suggest that rate-determining transition state involves interaction of $^1O_2$ with the π system of the aromatic rings, reacting in 4+2 cycloaddition reaction.[17,48,49] Furthermore, the oxazole LFER can be used to predict $^1O_2$ rate constants that cover a range of almost 2 orders of magnitude from the most reactive 2-methyloxazole (**2**) to the least reactive ester-substituted oxazole peptide (**13**, $k_{rxn}{}^{1O2}$ = 6.9 $\times 10^4$ $M^{-1}s^{-1}$). As it is experimentally difficult to measure such low $^1O_2$ rate constants, such an LFER approach proves useful for estimating the reactivity of electron poor oxazoles.

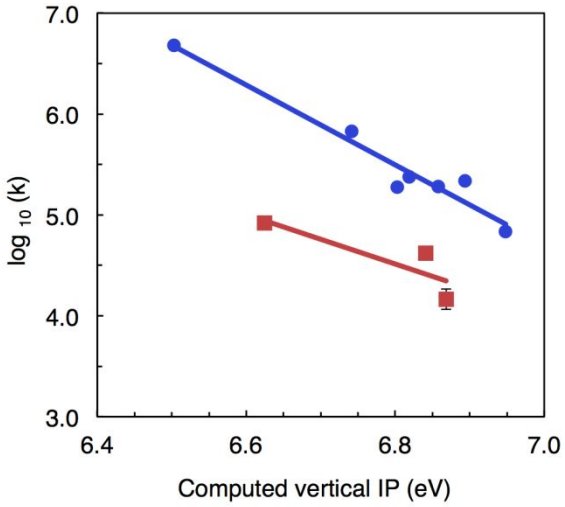

Figure 2. Linear free energy relationships (LFER) correlating calculated vertical ionization potentials (IP, eV) with $\log_{10} k_{rxn}$ values for the reaction of $^1O_2$ with oxazoles (blue circles) and thiazoles (red squares). The best fit lines have the following equations: $\log_{10} k_{rxn}$ (oxazole) = -3.96 × IP (eV) + 32.42, n = 7, r^2 = 0.95; $\log_{10} k_{rxn}$ (thiazole) = -2.45 × IP (eV) + 21.19, n = 3, r^2 = 0.73. The thiazole regression line includes only three time points, not completely sufficient to establish a good correlation, more work needs to be done in the future to extend this linear free energy relationship.

$^1O_2$ reaction products

We studied reaction products to help determine the reaction mechanism and to further understand the fate of such NRPs and RiPPs in aquatic environments. Previous studies report a triamide or a thioamide-diamide as major products from phenyl-substituted oxazoles and thiazoles.[19,49] Methoxazole **2** showed two major degradation products for the reaction with $^1O_2$ in H_2O. One of the products was confirmed to be a triamide, both from LC-HRMS and ^1H NMR analysis. The second major product was the imide proposed in Fig. 3. Following attack of $^1O_2$ on the aromatic ring and consequent Baeyer-Villiger-like rearrangement, **2** could undergo two different degradation pathways. The first pathway leads to the stable triamide, through a rearrangement of the intermediate imino anhydride (Fig. 3, purple pathway). In the second case, (Fig. 3, green pathway), the imino anhydride undergoes hydrolysis to produce an imide and acetic acid (confirmed by ^{13}C NMR and HSQC experiments, SI Fig. S32). After sensitized photolysis of peptide **1a** in H_2O the expected triamide was not detected. Instead, the major products were the imide shown in Fig. 3, identified by LC-HRMS, and formic acid, identified by ^1H NMR (Fig. 4 and see SI and Figure S30 and S31 for more details). These findings suggest that **1a** undergoes the same degradation pathway as **2** but forms an unstable triamide that hydrolyzes in water to the imide and formic acid (purple pathway, Fig. 3), consistent with the hydrolysis of formamides under mild conditions.[50] To further support the proposed reaction mechanisms, we performed the reaction in dry chloroform (absence of water). In this case, only the triamide was detected for both **1a** (Fig. 4) and **2**, but, after addition of water, we observed the formation of the imide and formic or acetic acid.

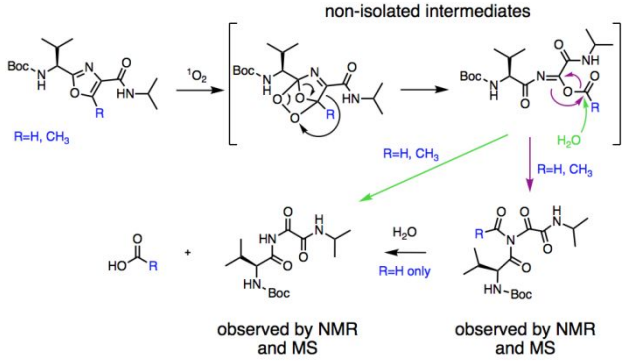

Figure 3. Degradation pathways of oxazole-containing peptides

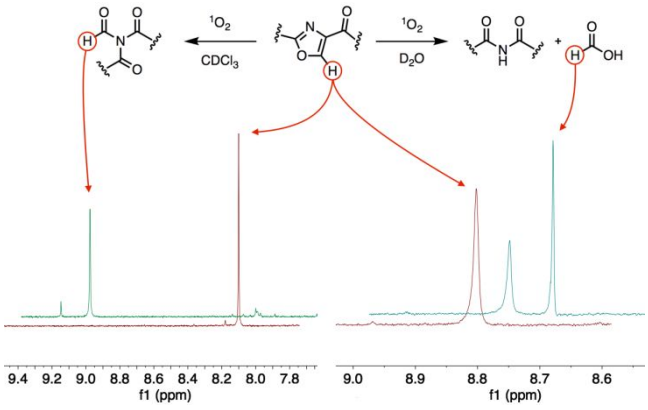

Figure 4. Left side: particular of the spectra of peptide **1a** at 0 min (red) and 120 min (green) in $CDCl_3$. The new peak at 9.1 ppm was assigned to the triamide proton. Right side: reaction of peptide **1a** in 50:50 CD_3CN:D_2O (at 0 min red spectrum,

and 340 min blue spectrum), at 8.80 pm the peak of **1a** and, shifted down field, the signal of formic acid.

Thiazole-peptide **3** behaves similarly to **2**, giving the same imide observed above and a thioamide-diamide, as products after reaction with $^1O_2$. These results are consistent with **3** undergoing an analogous reaction as **1a** and **2** and suggest that the hydrolysis of the thioamide-diamide is slower than for the triamide produced by peptide **1a**. In sum, the product studies indicate that peptide-based oxazoles and thiazoles react similarly to diaryl substituted oxazoles and thiazoles, and suggest that the triamide (or diamide-thioamide) and the imide products are diagnostic for reaction with $^1O_2$.

Conclusion.

In conclusion, we demonstrate that oxazoles and thiazoles stability increases when included in a peptide chain. Since they are known targets for reaction with $^1O_2$, and since $^1O_2$ is ubiquitious in sunlit waters, there would seem to be a negative selection pressure against the inclusion of these functional groups by organisms dwelling in the photic zone. This apparent paradox is resolved by the findings of the present work, which show that the carboxamide substitution greatly attenuates the reactivity of these heterocycles toward $^1O_2$. Overall, this study suggests also that these small peptide analogues of naturally occurring peptidic oxazoles and thiazoles are accessible and reasonable models to study the environmental photochemistry of more complex natural peptides.

Experimental

General. Unless otherwise indicated, all reagents were purchased from commercial distributors and used without further purification. Anhydrous solvents were freshly distilled from sodium benzophenone (THF) or CaH_2 (CH_2Cl_2), and stored over molecular sieves. Products were purified by flash chromatography on SiliaFlash P60 silica gel 40-63 µm (230-400 mesh, Silicycle Inc.). TLC was performed on SiliaPlate glass-backed TLC extra hard layer 60Å/UV254 (Silicycle Inc.). Preparative HPLC was performed on a SUPELCO Analytical Ascentis RP-AMIDE 10 cm x 21.2 mm, 5 µm column. ^{1}H and ^{13}C{^{1}H} NMR spectral data were recorded at 400 MHz and 100 MHz respectively on a Bruker Avance III 400 spectrometer. The chemical shifts were referenced to the corresponding residual solvent signal ($CDCl_3$: δH = 7.26 ppm, δC = 77.16 ppm; D_2O: δH = 4.79 ppm, δC MeOH in D_2O = 49.50 ppm). Data are reported as follows: chemical shift, multiplicity (s = singlet, d = doublet, t = triplet, q = quartet, p = pentet, m = multiplet, b = broad), integration, and coupling constants. High resolution ESI-mass spectra were obtained on a Thermo Exactive mass-spectrometer equipped with Orbitrap analyzer. UV-vis spectra were collected on a Cary 100 Biospec UV-vis spectrometer.

*Synthesis of (S)-3-hydroxy-1-methoxy-1-oxopropan-2-aminium chloride (**11**).* To a solution of L-serine (1070 mg, 10.2 mmol) in MeOH (15 mL) at 0 °C, $SOCl_2$ (4.3 mL, 59 mmol) was added dropwise over 15 min and the mixture was then refluxed for 3 h. The mixture was concentrated under vacuum to give **11** as a yellow solid (1592 mg, 100 %). ^{1}H NMR (400 MHz, D_2O) δ 4.30 (t, ^{1}H, J = 3.7 Hz), 4.15-4.00 (m, 2H), 3.89 (s, 1H); ^{13}C{^{1}H} NMR (100 MHz, D_2O) δ 169.5, 59.8, 55.3, 54.3. Characterization data were consistent with previous literature.[51]

*Synthesis of methyl (tert-butoxycarbonyl)-L-valyl-L-serinate (**12**).* A solution of Boc-val-OH (2.016 g, 9.3 mmol) and HOBt (190 mg, 1.4 mmol) in EtOH (45 mL) was stirred at room temperature for 15 minutes. To this was added a solution of L-serine methyl ester hydrochloride (1.588 g, 10.2 mmol) in EtOH (15 mL) and the mixture was cooled to 0-5 °C. *N*-methylmorpholine (3.28 mL, 30 mmol) was added over 5 minutes, and the reaction was stirred at 0-5 °C for 15 minutes. EDCI (1.97 mL, 11.2 mmol) was added in one portion, and the reaction mixture was allowed to reach room temperature overnight. The reaction was acidified with HCl 1 M and was reduced in vacuo. EtOAc (40 mL) was added, the mixture was vigorously shaken and the phases were separated. The organic phase was washed with pH 2 buffer (50 mL), water (50 mL), saturated aqueous $NaHCO_3$ solution (50 mL), and saturated aqueous NaCl solution (50 mL), dried over Na_2SO_4 and concentrated in vacuo to give dipeptide **12** as a yellow crystalline solid (1.04 g, 35 %). ^{1}H NMR (400 MHz, $CDCl_3$) δ 6.75 (d, *J* = 7.3 Hz, 1H), 5.05 (d, *J* = 8.4 Hz, 1H), 4.72 – 4.60 (m, 1H), 3.96 (s, 2H), 3.85 (t, *J* = 7.4 Hz, 1H), 3.80 (s, 3H), 2.83 (s, 1H), 2.19 – 2.06 (m, 1H), 1.44 (s, 9H), 0.98 (m, 6H); ^{13}C{^{1}H} NMR (100 MHz, $CDCl_3$) δ 172.2, 170.8, 156.3, 80.4, 63.0, 60.7, 54.9, 52.8, 30.9, 28.4, 19.3, 18.2. Characterization data were consistent with previous literature.[52]

*Synthesis of methyl (S)-2-(1-((tert-butoxycarbonyl)amino)-2-methylpropyl)oxazole-4-carboxylate (**13**).* Deoxo-Fluor (734 µL, 1.7 mmol) was added dropwise to a solution of **12** (500 mg, 1.57 mmol) in dry CH_2Cl_2 (14 mL) cooled to -20 °C (bath temperature). After 30 min, $BrCCl_3$ (560 µL, 5.7 mmol) was added dropwise to the reaction mixture, followed by DBU (850 µL, 5.7 mmol). The reaction was stirred at 2-3 °C for 8 h and then quenched with saturated aqueous sodium bicarbonate. The mixture was extracted with EtOAc, and the combined organic fractions were dried ($MgSO_4$), filtered, and concentrated. Purification of the residue by flash chromatography (2:1 hexane:ethyl acetate) gave **13** as a colorless solid (234 mg, 50 %). ^{1}H NMR (400 MHz, $CDCl_3$) δ 8.17 (s, 1H), 5.28 (d, 1H, J = 8 Hz), 4.81-4.77 (m, 1H), 3.91 (s, 3H), 2.23-2.15 (m, 1H), 1.42 (s, 9H), 0.93-0.90 (m, 6H); ^{13}C{^{1}H} NMR (100 MHz, $CDCl_3$) δ 165.3, 161.7, 155.5, 143.9, 133.3, 80.16, 54.4, 52.4, 33.1, 28.4, 18.8, 18.1. Characterization data were consistent with previous literature.[52]

*Synthesis of tert-butyl (S)-(1-(4-(isopropylcarbamoyl) oxazol-2-yl)-2 methylpropyl)carbamate (**1a**).* A solution of **13** (100 mg, 0.3 mmol) in isopropyl amine (3 mL) and water (0.2 mL) was stirred at room temperature for 48 h. The excess of isopropyl amine was removed under vacuum and ethyl acetate was added. The solution was dried over $MgSO_4$, filtered and concentrated under vacuum to give a yellow solid (109 mg, 100 %). ^{1}H NMR (400 MHz, $CDCl_3$) δ 8.10 (s, 1H), 6.70 (d, 1H, J = 7.1 Hz, broad), 5.08 (d, 1H, J = 9.2 Hz, broad), 4.76-4.72 (m, 1H), 4.29-4.17 (m, 1H), 2.21-2.13 (m, 1H), 1.45 (s, 9H), 1.24 (d, 6H, J = 6.5 Hz), 0.92 (dd, 6H, J1 = 6.8 Hz, J2 = 10.3 Hz); ^{13}C{^{1}H} NMR (100 MHz, $CDCl_3$) δ 163.7, 159.8, 155.4, 140.9, 136.4, 80.3, 54.6, 41.3, 32.8, 28.5, 22.9, 18.9, 18.2; ESI HRMS m/z calcd for $C_{16}H_{28}N_3O_4$ $[M + H]^+$:

326.2074, found: 326.2080; m/z calcd for $C_{16}H_{27}N_3O_4Na$ [M + Na]$^+$: 348.1894, found: 348.1902.

*Synthesis of methyl (tert-butoxycarbonyl)glycyl-L-serinate (**17**).* The reaction was performed as described in the procedure for compound **12** to furnish **17** in 30% yield (356 mg): ^{1}H NMR (400 MHz, $CDCl_3$) δ 7.01 (d, J = 7.5 Hz, 1H), 5.24 (s, 1H), 4.67 (m, 1H), 3.97 (m, 2H), 3.84 (d, J = 5.8 Hz, 2H), 3.79 (s, 3H), 2.85 (t, J = 6.3 Hz, 1H), 1.46 (s, 9H); ^{13}C{^{1}H} NMR (100 MHz, $CDCl_3$) δ 170.8, 169.84, 156.4, 80.9, 63.1, 54.9, 52.9, 44.6, 28.4. Characterization data were consistent with previous literature.[53]

*Synthesis of methyl 2-(((tert-butoxycarbonyl)amino) methyl)oxazole-4-carboxylate (**18**).* The reaction was performed as described in the procedure for compound **13** to furnish **18** in 55% yield (181 mg): ^{1}H NMR (400 MHz, $CDCl_3$) δ 8.19 (s, 1H), 5.18 (s, 1H, b), 4.50 (d, J = 5.9 Hz, 2H), 3.92 (s, 3H), 1.45 (s, 9H); ^{13}C{^{1}H} NMR (100 MHz, $CDCl_3$) δ 162.4, 161.6, 155.6, 144.4, 133.5, 80.6, 52.4, 38.1, 28.4. Characterization data were consistent with previous literature.[53]

*Synthesis of tert-butyl ((4-(isopropylcarbamoyl)oxazol-2-yl)methyl)carbamate (**1b**).* The reaction was performed as described in the procedure for compound **1a** to furnish **1b** in 100% yield (200 mg). Crude **1b** was then purified by prep-HPLC (70:30 CH_3CN:H_2O). ^{1}H NMR (400 MHz, $CDCl_3$) δ 8.11 (s, 1H), 6.69 (d, J = 8.0 Hz, 1H), 5.12 (s, 1H, b), 4.43 (d, J = 5.9 Hz, 2H), 4.23 (m, 1H), 1.46 (s, 9H), 1.24 (d, J = 6.6 Hz, 6H); ^{13}C{^{1}H} NMR (100 MHz, $CDCl_3$) δ 161.1, 159.6, 155.58, 141.3, 136.7, 80.7, 41.2, 38.2, 28.5, 22.9. ESI HRMS *m/z* calcd for $C_{13}H_{21}N_3O_4Na$ [M + Na]$^+$: 306.1424, found: 306.1420.

*Synthesis of methyl (tert-butoxycarbonyl)-L-phenylalanyl-L-serinate (**19**).* The reaction was performed as described in the procedure for compound **12** to furnish **19** in 42% yield (487 mg): ^{1}H NMR (400 MHz, $CDCl_3$) δ 7.36 – 7.14 (m, 5H), 6.79 (d, J = 7.3 Hz, 1H), 5.02 (d, J = 7.3 Hz, 1H), 4.60-4.57 (m, 1H), 4.32 (q, J = 7.0 Hz, 1H), 4.00 – 3.82 (m, 2H), 3.75 (s, 3H), 3.14-3.04 (m, 2H), 1.40 (s, 9H); ^{13}C{^{1}H} NMR (100 MHz, $CDCl_3$) δ 171.7, 170.5, 155.8, 136.5, 129.4, 128.9, 127.2, 80.8, 62.9, 56.3, 55.1, 52.9, 38.0, 28.4. Characterization data were consistent with previous literature.[53]

*Synthesis of methyl (S)-2-(1-((tert-butoxycarbonyl)amino)-2-phenylethyl)oxazole-4-carboxylate (**20**).* The reaction was performed as described in the procedure for compound **13** to furnish **20** in 57% yield (262 mg): ^{1}H NMR (400 MHz, $CDCl_3$) δ 8.12 (s, 1H), 7.25-7.19 (m, 3H), 7.03 (d, J = 7.0 Hz, 2H), 5.21 (s, 2H, b), 3.91 (s, 3H), 3.25 – 3.21 (m, 2H), 1.40 (s, 9H); ^{13}C{^{1}H} NMR (100 MHz, $CDCl_3$) δ 164.9, 161.6, 155.0, 144.0, 135.7, 133.5, 129.4, 128.8, 127.2, 80.4, 52.4, 50.3, 40.6, 28.4. Characterization data were consistent with previous literature.[53]

*Synthesis of tert-butyl (S)-(1-(4-(isopropylcarbamoyl) oxazol-2-yl)-2-phenylethyl) carbamate (**1c**).* The reaction was performed as described in the procedure for compound **1a** to furnish **1c** in 100% yield (282 mg). Crude **1c** was then purified by prep-HPLC (70:30 CH_3CN:H_2O). ^{1}H NMR (400 MHz, $CDCl_3$) δ 8.02 (s, 1H), 7.19 – 7.12 (m, 3H), 7.01 – 6.87 (m, 2H), 6.57 (d, J = 8.2 Hz, 1H), 5.09 (s, 1H, b), 4.98 (s, 1H, b), 4.19 – 4.11 (m, 1H), 3.19 – 3.14 (m, 3H), 1.35 (s, 9H), 1.17 (d, J = 6.6 Hz, 6H); ^{13}C{^{1}H} NMR (100 MHz, $CDCl_3$) δ 163.3, 159.7, 155.0, 141.0, 136.5, 135.7, 129.4, 128.8, 127.3, 80.5, 50.3, 41.3, 40.1, 28.4, 22.9. ESI HRMS *m/z* calcd for $C_{20}H_{27}N_3O_4Na$ [M + Na]$^+$: 396.1894, found: 396.1884.

*Synthesis of (2S,3R)-3-hydroxy-1-methoxy-1-oxobutan-2-aminium chloride (**14**).* The reaction was performed as described in the procedure for compound **11** to furnish **14** as a yellow thick oil (1463 mg, 100% yield). ^{1}H NMR (400 MHz, D_2O) δ 4.48-4.42 (m, 1H), 4.13 (d, 1H, J = 4 Hz), 3.88 (s, 3H), 1.36 (d, 3H, J = 4 Hz); ^{13}C{^{1}H} NMR (100 MHz, D_2O) δ 169.9, 65.9, 59.0, 54.4, 19.4. Characterization data were consistent with previous literature.[54]

*Synthesis of methyl (tert-butoxycarbonyl)-L-valyl-L-allothreoninate (**15**).* The reaction was performed as described in the procedure for compound **12** in the main text to furnish **15** in 96% yield (1265 mg): ^{1}H NMR (400 MHz, $CDCl_3$) δ 6.78 (d, 1H, J = 8 Hz), 4.62 (dd, 1H, J_1 = 4 Hz, J_1 = 8 Hz), 4.37-4.35 (m, 1H), 3.96-3.92 (m, 1H), 3.77 (s, 3H), 2.91 (s, 1H), 2.13-2.08 (m, 1H), 1.43 (s, 9H), 1.20 (d, 3H, J = 4 Hz), 0.99 (d, 3H, J = 8 Hz), 0.96 (d, 3H, J = 8 Hz); ^{13}C{^{1}H} NMR (100 MHz, $CDCl_3$) δ 172.4, 171.4, 156.2, 80.2, 68.3, 57.4, 52.7, 30.9, 28.4, 20.1, 19.3, 18.2. Characterization data were consistent with previous literature.[55]

*Synthesis of methyl (S)-2-(1-((tert-butoxycarbonyl)amino)-2-methylpropyl)-5 methyloxazole-4-carboxylate (**16**).* The reaction was performed as described in the procedure for compound **13** to furnish **16** in 44% yield (291 mg): ^{1}H NMR (400 MHz, $CDCl_3$) δ 5.27 (d, J = 9.5 Hz, 1H), 4.75 (t, J = 7.9 Hz, 1H), 3.93 (s, 3H), 2.63 (s, 3H), 2.21-2.16 (m, 1H), 1.46 (s, 9H), 0.95 (m, 6H); ^{13}C{^{1}H} NMR (100 MHz, $CDCl_3$) δ 162.9, 162.3, 156.4, 156.0, 127.4, 80.1, 54.3, 52.1, 33.1, 28.5, 19.0, 18.1, 12.2. Characterization data were consistent with previous literature.[55]

*Synthesis of tert-butyl (S)-(1-(4-(isopropylcarbamoyl)-5-methyloxazol-2-yl)-2 methylpropyl)carbamate (**2**).* The reaction was performed as described in the procedure for compound **1a**. The crude product was obtained in 100% yield (65 mg) and then purified by prep-HPLC (70:30 CH_3CN:H_2O) to furnish **2**: ^{1}H NMR (400 MHz, $CDCl_3$) δ 6.73 (d, J = 8.2 Hz, 1H), 5.06 (d, J = 9.3 Hz, 1H), 4.67 (m, 1H), 4.26-4.16 (m, 1H), 2.61 (s, 3H), 2.15 (m, 1H), 1.46 (s, 9H), 1.24 (d, J = 6.4 Hz, 6H), 0.93 (t, J = 6.8 Hz, 6H); ^{13}C{^{1}H} NMR (100 MHz, $CDCl_3$) δ 161.3, 160.7, 155.5, 152.8, 129.2, 80.2, 54.4, 41.0, 32.8, 28.5, 23.0, 18.9, 18.1, 11.8. ESI HRMS *m/z* calcd for $C_{17}H_{29}N_3O_4$-H [M + H]$^+$: 340.2231, found: 340.2238; *m/z* calcd for $C_{17}H_{29}N_3O_4Na$ [M + Na]$^+$: 362.2050, found: 362.2059.

*Synthesis of tert-butyl (S)-(1-amino-3-methyl-1-oxobutan-2-yl)carbamate (**21**).* To a solution of Boc-valine-OH (3 g, 13.8 mmol) and *N*-methylmorpholine (1.82 mL, 16.5 mmol) in DME (65 mL) was added isobutyl chloroformate (2.15 mL, 16.5 mmol) dropwise at 0 °C under inert atmosphere (N_2). The resulting mixture was stirred at 0 °C for 2 min, and a solution of ammonia (30 % w/w aqueous solution, 5.3 mL) was then added. The resulting white slurry was vigorously stirred at room temperature for 1 h and quenched with water. CH_2Cl_2 (40 mL) was added, the organic layer was separated, and the aqueous layer was extracted with CH_2Cl_2 (3 x 30 mL).

Combined organic fractions were successively washed with a 1 M HCl aqueous solution and brine, dried over MgSO4, filtered, and concentrated under vacuum to yield the desired amide as a white solid (2.81 g, 13.0 mmol, 94 %): ^{1}H NMR (400 MHz, $CDCl_3$) δ 5.88 (s, 1H, broad), 5.41 (s, 1H, broad), 5.01 (s, 1H, broad), 3.97-3.94 (m, 1H), 2.20-2.14 (m, 1H), 1.45 (s, 9H), 1.00-0.92 (m, 6H); ^{13}C{^{1}H} NMR (100 MHz, $CDCl_3$) δ 174.1, 156.1, 59.6, 30.8, 28.5, 19.4, 17.8. Characterization data were consistent with previous literature.[55]

*Synthesis of tert-butyl (S)-(1-amino-3-methyl-1-thioxobutan-2-yl)carbamate (**22**).* Lawesson's reagent (4.04 g, 10 mmol) was added to a solution of Boc-Val-NH_2 (2.81 g, 13.0 mmol) in dry THF (110 mL) at 0 °C under inert atmosphere (N_2). The solution was warmed to room temperature, stirred for 5 h and then filtered. The mother liquor was partitioned between saturated aqueous $NaHCO_3$ (150 mL) and ether. The aqueous phase was extracted with ether (3 x 50 mL). The organic layers were combined, washed with brine (70 mL), dried over Na_2SO_4 and concentrated to give a yellow solid (2.84 g, 12.2 mmol, 94 %): ^{1}H NMR (400 MHz, $CDCl_3$) δ 7.67 (s, 1H, broad), 7.51 (s, 1H, broad), 5.20 (s, 1H, broad), 4.16-4.12 (m, 1H), 2.25 (s, 1H, broad), 1.44 (s, 9H), 1.00-0.92 (m, 6H); ^{13}C{^{1}H} NMR (100 MHz, $CDCl_3$) δ 209.6, 156.0, 65.8, 33.1, 28.5, 19.9, 19.1. Characterization data were consistent with previous literature.[56]

*Synthesis of ethyl (S)-2-(1-((tert-butoxycarbonyl)amino)-2-methylpropyl)thiazole-4-carboxylate (**23**).* Ethyl bromopyruvate (4.6 mL, 36.6 mmol) was added to a suspension of $KHCO_3$ (9.77 g) and **22** (2.84 g, 12.2 mmol) which had been stirred in dry DME (35 mL) at -15 °C under inert atmosphere (N_2) for 5 min. After 1 min, the mixture was treated with a solution of 2,6-lutidine (12.2 mL, 105 mmol) and trifluoroacetic acid (1.7 mL, 12.2 mmol) in dry DME (25 mL) at -15 °C. The reaction mixture was stirred for 10 h at the same temperature, poured into water (60 mL) and extracted with CH_2Cl_2. The organic layers were combined, dried over Na_2SO_4 and concentrated. The residue was purified by column chromatography (ethyl acetate/petroleum ether, 1:4) to give a yellow solid (1.00 g, 3.05 mmol, 25 %): ^{1}H NMR (400 MHz, $CDCl_3$) δ 8.07 (s, 1H), 5.28 (d, J = 9.1 Hz, 1H), 4.90 (m, 1H), 4.41 (q, J = 7.1 Hz, 2H), 2.45 – 2.42 (m, 1H), 1.45 (s, 9H), 1.40 (t, J = 7.1 Hz, 4H), 0.98 (d, J = 6.8 Hz, 3H), 0.90 (d, J = 6.8 Hz, 3H); ^{13}C{^{1}H} NMR (100 MHz, $CDCl_3$) δ 173.3, 161.5, 155.6, 147.6, 126.7, 80.2, 61.6, 58.2, 33.5, 28.5, 19.6, 17.4, 14.5. Characterization data were consistent with previous literature.[57]

*Synthesis of tert-butyl (S)-(1-(4-(isopropylcarbamoyl) thiazol-2-yl)-2-methylpropyl)carbamate (**3**).* A solution of **23** (300 mg, 0.91 mmol) in isopropyl amine (3 mL) and water (0.2 mL) was stirred at room temperature for 48 h. The excess of isopropyl amine was removed under vacuum and ethyl acetate was added. The solution was dried with $MgSO_4$, filtered and concentrated in vacuum to give a yellow solid (310 mg, 100 %). The crude product was then purified by prep-HPLC (70:30 CH_3CN:H_2O) to afford **3** as a white solid (280 mg). ^{1}H NMR (400 MHz, $CDCl_3$) δ 7.98 (s, 1H), 7.08 (d, J = 8.3 Hz, 1H), 5.12 (d, J = 9.0 Hz, 1H), 4.86 (m, 1H), 4.25 (dp, J = 8.1, 6.5 Hz, 1H), 2.34 (m, 1H), 1.46 (s, 9H), 1.27 (d, J = 6.5 Hz, 6H), 0.99 (d, J = 6.8 Hz, 3H), 0.93 (d, J = 6.8 Hz, 3H); ^{13}C{^{1}H} NMR (100 MHz, $CDCl_3$) δ 172.7, 160.4, 155.5, 150.6, 122.5, 80.4, 58.2, 41.5, 33.5, 28.5, 23.0, 19.5, 17.6. ESI HRMS m/z calcd for $C_{16}H_{28}N_3O_3S$ $[M + H]^+$: 342.1846, found: 342.1844; m/z calcd for $C_{16}H_{27}N_3O_3SNa$ $[M + Na]^+$: 364.1665, found: 364.1663.

*Synthesis of N-isopropyl-2-methyloxazole-4-carboxamide (**6**).* The reaction was performed as described in the procedure for compound **1a**, starting from commercially available methyl 2-methyloxazole-4-carboxylate (**24**), to furnish **6** in 100% yield (519 mg), ^{1}H NMR (400 MHz, $CDCl_3$) δ 8.05 (s, 1H), 6.68 (s, 1H), 4.23 (dp, J = 8.3, 6.6 Hz, 1H), 2.46 (s, 3H), 1.24 (d, J = 6.6 Hz, 6H); ^{13}C{^{1}H} NMR (100 MHz, $CDCl_3$) δ 161.3, 160.0, 140.8, 136.6, 41.1, 22.9, 13.9. ESI HRMS *m/z* calcd for $C_8H_{13}N_2O_2$ $[M + H]^+$: 169.0972, found: 169.0971; *m/z* calcd for $C_8H_{12}N_2O_2Na$ $[M + Na]^+$: 191.0791, found: 191.0795.

*Synthesis of N-isopropyl-2-methylthiazole-4-carboxamide (**8**).* The reaction was performed as described in the procedure for compound **1a**, starting from commercially available ethyl 2-methylthiazole-4-carboxylate, to give **8** as a yellow solid in 100% yield (1044 mg), ^{1}H NMR (400 MHz, $CDCl_3$) δ 7.90 (s, 1H), 7.13 (s, 1H, broad), 4.24 dp, J = 8.0, 6.5 Hz, 1H), 2.69 (s, 3H), 1.25 (d, 6H, J=6.6 Hz); ^{13}C{^{1}H} NMR (100 MHz, $CDCl_3$) δ 165.9, 160.4, 150.2, 122.7, 41.4, 22.9, 19.2. ESI HRMS *m/z* calcd for $C_8H_{13}N_2OS$ $[M + H]^+$: 185.0743, found: 185.0747; *m/z* calcd for $C_8H_{12}N_2OSNa$ $[M + Na]^+$: 207.0563, found: 207.0566.

*Synthesis of N-isopropyl-2,5-dimethylfuran-3-carboxamide (**10**).* Dry CH_2Cl_2 (10 mL) and TEA (290 □L, 2.1 mmol) were added to isopropyl amine (195 □L, 2.3 mmol) under an N_2 atmosphere and the mixture was cooled at 0 °C. 2,5-dimethylfuran-3-carbonyl chloride (252 □L, 1.9 mmol) was added dropwise and then the cooling bath was removed. The reaction mixture was stirred at rt for 3 h and then washed with saturated aqueous $NaHCO_3$ (10 mL). The aqueous layer was extracted with CH_2Cl_2 (3x10 mL) and the organic phase was combined, dried over $MgSO_4$, filtered and concentrated in vacuo to give **10** (300 mg, 87 %): ^{1}H NMR (400 MHz, $CDCl_3$) δ 5.98 (s, 1H), 5.41 (s, 1H), 4.23 (dp, J = 7.8, 6.5 Hz, 1H), 2.55 (s, 3H), 2.26 (s, 3H), 1.23 (d, J = 6.5 Hz, 6H). ^{13}C{^{1}H} NMR (100 MHz, $CDCl_3$) δ 163. 5, 155.1, 150.0, 116.3, 104.1, 41.2, 23.1, 13.6, 13.4. ESI HRMS *m/z* calcd for $C_{10}H_{16}NO_2$ $[M + H]^+$: 182.1176, found: 182.1177; *m/z* calcd for $C_{10}H_{15}NO_2Na$ $[M + Na]^+$: 204.0995, found: 204.0998. Characterization data were consistent with previous literature.[58]

Direct photolysis of oxazole and thiazole compounds. Direct photolysis experiments were performed in borosilicate test tubes that contained the compounds at an initial concentration of 10 μM and phosphate buffer at pH 7. The photochemical reactions were performed at 300 nm and at 365 nm using 8 light bulbs at a distance of 5 cm from the samples, no filters were employed (see SI for lamp spectra).

Photolysis of oxazole and thiazole compounds in the presence of $^1O_2$. Sensitized photolysis experiments were performed in separate experimental setups and contained the compounds at an initial concentration of 10 μM, phosphate buffer at pH 7, furfuryl alcohol (FFA, 100 μM), and perinaphthenone (5 μM), as the $^1O_2$ sensitizer. The experiments were performed in borosilicate test tubes using 8

light bulbs with peak emission at 365 nm at a distance of 5 cm from the samples, no filters were employed. The experiments were performed in 100% H_2O and 80% D_2O 20% H_2O to enhance the steady-state concentration of $^1O_2$. Aliquots of 80 µL were taken at set time points and analyzed for FFA and oxazole or thiazole concentrations using ultra high-pressure liquid chromatography (UPLC, Waters ACQUITY) coupled with a photodiode array detector. FFA was used as a probe to determine the steady-state $^1O_2$ concentration in the bulk aqueous phase. Then, steady-state $^1O_2$ concentrations were obtained by dividing the pseudo-first-order rate constant of FFA degradation by its reaction rate constant with $^1O_2$ ($k_{rxn}^{FFA} = 1 \times 10^8$ $M^{-1}s^{-1}$).[59] The second-order reaction rate constants (k_{rxn}, $M^{-1}s^{-1}$) of model peptides were calculated by dividing each pseudo-first-order photo-transformation rate constant by the FFA-measured $^1O_2$ concentration, representing the intrinsic bimolecular rate constants.

Computational method. Density Functional Theory (DFT) molecular orbital calculations were performed using the Gaussian 09 program32,[60] on a 1215 compute nodes - Hewlett-Packard m710x, each equipped with a quad-core Intel Xeon E3-1285Lv5 processor. Geometries of the molecules considered in this study were optimized by using gradient corrected DFT with Minnesota global hybrid functional with 54% Hartree-Fock exchange (M06-2X) and with the 6-31G+(d) basis set. Analytic second derivative calculations, which yielded positive harmonic vibrational frequencies, were performed at the optimized geometries to ensure that the optimized geometries were minima on the potential energy surface. The optimized structures were then submitted for single-point energy calculations performed using the M06-2X functional with the larger basis set jun-cc-pVTZ. All energies and geometries were calculated in water using the solvation model SMD, which has been shown to represent solution-phase species.[61] Furthermore, the vertical ionization potentials from the bottom of the potential well of the neutral system were calculated and used as a proxy for quantifying the electronic character on the oxazole and thiazole rings.

ASSOCIATED CONTENT

Supporting Information

The supporting information is available free of charge on the ACS Publications website at DOI:

^1H NMR, $^{13}C\{^1H\}$NMR and UV-vis spectra of model peptides, photolysis experiments details, selected optimized geometries and product identification details are included in the supportive information (PDF).

AUTHOR INFORMATION

Corresponding Author

* kristopher.mcneill@env.ethz.ch

Notes

The authors declare no competing financial interest.

ACKNOWLEDGMENT

We acknowledge Dr. Cyril Portmann (EPFL), Dr. Simon Sieber (UZH) and Prof. Karl Gademann (UZH) for supplying Aerucyclamide A, Dr. Gordon Getzinger (ETH Zürich) for helpful MS discussions, Dr. Peter Tentscher (Eawag) for helpful Gaussian discussions. We gratefully acknowledge support from the Swiss National Science Foundation (Grant number 200021_138008).

ABBREVIATIONS

NRPs, nonribosomal peptides.
RiPPs, ribosomally synthesized and post-translationally modified peptides.
EWG, electron withdrawing group.
EDCI, 1-Ethyl-3-(3-dimethylaminopropyl)carbodiimide.
DBU, 1,8-Diazabicyclo[5.4.0]undec-7-ene.
HOBt, Hydroxybenzotriazole.
Boc, tert-butyloxycarbonyl

Reference

(1) Roy, R. S.; Gehring, A. M.; Milne, J. C.; Belshaw, P. J.; Walsh, C. T. Thiazole and Oxazole Peptides: Biosynthesis and Molecular Machinery. *Nat. Prod. Rep.* **1999**, *16*, 249–263.

(2) Jin, Z. Muscarine, Imidazole, Oxazole and Thiazole Alkaloids. *Nat. Prod. Rep.* **2016**, *33*, 1268–1317.

(3) Admi, V.; Afek, U.; Carmeli, S. Raocyclamides A and B, Novel Cyclic Hexapeptides Isolated from the Cyanobacterium Oscillatoria Raoi. *J. Nat. Prod.* **1996**, *59*, 396–399.

(4) Dalisay, D. S.; Rogers, E. W.; Edison, A. S.; Molinski, T. F. Structure Elucidation at the Nanomole Scale. 1. Trisoxazole Macrolides and Thiazole-Containing Cyclic Peptides from the Nudibranch *Hexabranchus Sanguineus*. *J. Nat. Prod.* **2009**, *72*, 732–738.

(5) Tan, L. T.; Williamson, R. T.; Gerwick, W. H.; Watts, K. S.; McGough, K.; Jacobs, R. *Cis,Cis* - and *Trans,Trans* - Ceratospongamide, New Bioactive Cyclic Heptapeptides from the Indonesian Red Alga *Ceratodictyon s Pongiosum* and Symbiotic Sponge *Sigmadocia s Ymbiotica*. *J. Org. Chem.* **2000**, *65*, 419–425.

(6) Mau, C. M. S.; Nakao, Y.; Yoshida, W. Y.; Scheuer, P. J.; Kelly-Borges, M. Waiakeamide, a Cyclic Hexapeptide from the Sponge Ircinia Dendroides1. *J. Org. Chem.* **1996**, *61* (18), 6302–6304. https://doi.org/10.1021/jo960771e.

(7) Rashid, M. A.; Gustafson, K. R.; Boswell, J. L.; Boyd, M. R. Haligramides A and B, Two New Cytotoxic Hexapeptides from the Marine Sponge Haliclona Nigra. *J. Nat. Prod.* **2000,** *63,* 956-959.

(8) Williams, P. G.; Yoshida, W. Y.; Moore, R. E.; Paul, V. J. Isolation and Structure Determination of Obyanamide, a Novel Cytotoxic Cyclic Depsipeptide from the Marine Cyanobacterium *Lyngbya Confervoides*. *J. Nat. Prod.* **2002**, *65*, 29–31.

(9) Tan, L. T.; Sitachitta, N.; Gerwick, W. H. The Guineamides, Novel Cyclic Depsipeptides from a Papua New Guinea Collection of the Marine Cyanobacterium *Lyngbya m Ajuscula*. *J. Nat. Prod.* **2003**, *66*, 764–771.

(10) Singh, E. K.; Ramsey, D. M.; McAlpine, S. R. Total Synthesis of *Trans*, *Trans*- Sanguinamide B and Conformational Isomers. *Org. Lett.* **2012**, *14*, 1198–1201.

(11) Portmann, C.; Sieber, S.; Wirthensohn, S.; Blom, J. F.; Da Silva, L.; Baudat, E.; Kaiser, M.; Brun, R.; Gademann, K. Balgacyclamides, Antiplasmodial Heterocyclic Peptides from *Microcystis Aeruginosa* EAWAG 251. *J. Nat. Prod.* **2014**, *77*, 557–562.

(12) Wick, L. Y.; McNeill, K.; Rojo, M.; Medilanski, E.; Gschwend, P. M. Fate of Benzene in a Stratified Lake Receiving Contaminated Groundwater Discharges from a

Superfund Site. *Environ. Sci. Technol.* **2000**, *34*, 4354–4362.
(13) Wolff, C. J. M.; Halmans, M. T. H.; van der Heijde, H. B. The Formation of Singlet Oxygen in Surface Waters. *Chemosphere* **1981**, *10*, 59–62.
(14) Zepp, R. G.; Wolfe, N. L.; Baughman, G. L.; Hollis, R. C. Singlet Oxygen in Natural Waters. *Nature* **1977**, *267*, 421–423.
(15) Helz, G. R.; Zepp, R. G.; Crosby, D. G. Aquatic and Surface Photochemistry. Taylor and Francis Group, **1994** CRC Press, Inc.
(16) Usui, Y.; Tsukada, M.; Nakamura, H. Kinetic Studies of Photosensitized Oxygenation by Singlet Oxygen in Aqueous Micellar Solutions. *Bull. Chem. Soc. Jpn.* **1978**, *51*, 379–384.
(17) H. Wasserman, H.; E. Pickett, J.; S. Vinnick, F. Intermediates in the Reactions of Oxazoles with Singlet Oxygen. *Heterocycles* **1981**, *15*, 1069.
(18) Vatansever, F.; de Melo, W. C. M. A.; Avci, P.; Vecchio, D.; Sadasivam, M.; Gupta, A.; Chandran, R.; Karimi, M.; Parizotto, N. A.; Yin, R.; et al. Antimicrobial Strategies Centered around Reactive Oxygen Species – Bactericidal Antibiotics, Photodynamic Therapy, and Beyond. *FEMS Microbiol. Rev.* **2013**, *37*, 955–989.
(19) Matsuura, T.; Saito, I. Photoinduced Reactions. XXXIV. Photosensitized Oxygenation of 2,4,5-Triphenylthiazole. *Bull. Chem. Soc. Jpn.* **1969**, *42*, 2973–2975.
(20) Swellmeen, L. 1, 3-Oxazole Derivatives: A Review of Biological Activities as Antipathogenic Lubna Swellmeen. *Pharma Chem.* **2016**, *8*, 269–286.
(21) McGrath, N. A.; Brichacek, M.; Njardarson, J. T. A Graphical Journey of Innovative Organic Architectures That Have Improved Our Lives. *J. Chem. Educ.* **2010**, *87*, 1348–1349.
(22) Hamada, Y.; Shibata, M.; Shioiri, T. New Methods and Reagents in Organic Synthesis. 58: A Synthesis of Patellamide a, a Cytotoxic Cyclic Peptide from a Tunicate. Revision of Its Proposed Structure. *Tetrahedron Lett.* **1985**, *26*, 6501–6504.
(23) Cavelier-Frontin, F.; Pepe, G.; Verducci, J.; Siri, D.; Jacquier, R. Prediction of the Best Linear Precursor in the Synthesis of Cyclotetrapeptides by Molecular Mechanic Calculations. *J. Am. Chem. Soc.* **1992**, *114*, 8885–8890.
(24) Ireland, C. M.; Durso, A. R.; Newman, R. A.; Hacker, M. P. Antineoplastic Cyclic Peptides from the Marine Tunicate Lissoclinum Patella. *J. Org. Chem.* **1982**, *47*, 1807–1811.
(25) McDonald, L. A.; Foster, M. P.; Phillips, D. R.; Ireland, C. M.; Lee, A. Y.; Clardy, J. Tawicyclamides A and B, New Cyclic Peptides from the Ascidian Lissoclinum Patella: Studies on the Solution- and Solid-State Conformations. *J. Org. Chem.* **1992**, *57*, 4616–4624.
(26) Portmann, C.; Blom, J. F.; Kaiser, M.; Brun, R.; Jüttner, F.; Gademann, K. Isolation of Aerucyclamides C and D and Structure Revision of Microcyclamide 7806A: Heterocyclic Ribosomal Peptides from *Microcystis Aeruginosa* PCC 7806 and Their Antiparasite Evaluation. *J. Nat. Prod.* **2008**, *71*, 1891–1896.
(27) Foster, M. P.; Concepcion, G. P.; Caraan, G. B.; Ireland, C. M. Bistratamides C and D. Two New Oxazole-Containing Cyclic Hexapeptides Isolated from a Philippine Lissoclinum Bistratum Ascidian. *J. Org. Chem.* **1992**, *57*, 6671–6675.
(28) Linington, R. G.; González, J.; Ureña, L.-D.; Romero, L. I.; Ortega-Barría, E.; Gerwick, W. H. Venturamides A and B: Antimalarial Constituents of the Panamanian Marine Cyanobacterium *Oscillatoria* Sp. ⊥. *J. Nat. Prod.* **2007**, *70*, 397–401.
(29) Todorova, A. K.; Juettner, F.; Linden, A.; Pluess, T.; von Philipsborn, W. Nostocyclamide: A New Macrocyclic, Thiazole-Containing Allelochemical from Nostoc Sp. 31 (Cyanobacteria). *J. Org. Chem.* **1995**, *60*, 7891–7895.
(30) Degnan, B. M.; Hawkins, C. J.; Lavin, M. F.; McCaffrey, E. J.; Parry, D. L.; Watters, D. J. Novel Cytotoxic Compounds from the Ascidian Lissoclinum Bistratum. *J. Med. Chem.* **1989**, *32*, 1354–1359.
(31) Perez, L. J.; Faulkner, D. J. Bistratamides E−J, Modified Cyclic Hexapeptides from the Philippines Ascidian *Lissoclinum b Istratum*. *J. Nat. Prod.* **2003**, *66*, 247–250.
(32) Anderson, Z. J.; Fox, D. J. Total Synthesis of the Azolemycins. *Org. Biomol. Chem.* **2016**, *14*, 1450–1454.
(33) Phillips, A. J.; Uto, Y.; Wipf, P.; Reno, M. J.; Williams, D. R. Synthesis of Functionalized Oxazolines and Oxazoles with DAST and Deoxo-Fluor. *Org. Lett.* **2000**, *2*, 1165–
(34) Toumi, M.; Couty, F.; Evano, G. Total Synthesis of the Cyclopeptide Alkaloid Paliurine E. Insights into Macrocyclization by Ene−Enamide RCM. *J. Org. Chem.* **2008**, *73*, 1270–1281.
(35) Wu, W.; Li, Z.; Zhou, G.; Jiang, S. Total Synthesis of Argyrins A and E. *Tetrahedron Lett.* **2011**, *52*, 2488–2491.
(36) McNeill, K.; Canonica, S. Triplet State Dissolved Organic Matter in Aquatic Photochemistry: Reaction Mechanisms, Substrate Scope, and Photophysical Properties. *Environ. Sci. Process. Impacts* **2016**, *18*, 1381–1399.
(37) Segado, M.; Reguero, M. Mechanism of the Photochemical Process of Singlet Oxygen Production by Phenalenone. *Phys. Chem. Chem. Phys.* **2011**, *13*, 4138.
(38) Foote, C. S.; Clennan, E. L. Properties and Reactions of Singlet Dioxygen. In *Active Oxygen in Chemistry*; Foote, C. S., Valentine, J. S., Greenberg, A., Liebman, J. F., Eds.; Structure Energetics and Reactivity in Chemistry Series; Springer Netherlands: Dordrecht, 1995; pp 105–140.
(39) Boger, D. L. Diels-Alder Reactions of Heterocyclic Aza Dienes. Scope and Applications. *Chem. Rev.* **1986**, *86*, 781–793.
(40) Gollnick, K.; Griesbeck, A. Singlet Oxygen Photooxygenation of Furans. *Tetrahedron* **1985**, *41*, 2057–2068.
(41) Montagnon, T.; Kalaitzakis, D.; Triantafyllakis, M.; Stratakis, M.; Vassilikogiannakis, G. Furans and Singlet Oxygen – Why There Is More to Come from This Powerful Partnership. *Chem Commun* **2014**, *50*, 15480–15498.
(42) Wipf, P. Synthetic Studies of Biologically Active Marine Cyclopeptides. *Chem. Rev.* **1995**, *95*, 2115–2134.
(43) Moody, C. J.; Bagley, M. C. Total Synthesis of (+)-Nostocyclamide. *J. Chem. Soc., Perkin Trans. 1* **1998**, 601-607.
(44) Davyt, D.; Serra, G. Thiazole and Oxazole Alkaloids: Isolation and Synthesis. *Mar. Drugs* **2010**, *8*, 2755–2780.
(45) Portmann, C.; Blom, J. F.; Gademann, K.; Jüttner, F. Aerucyclamides A and B: Isolation and Synthesis of Toxic Ribosomal Heterocyclic Peptides from the Cyanobacterium *Microcystis Aeruginosa* PCC 7806. *J. Nat. Prod.* **2008**, *71*, 1193–1196.
(46) Koopmans, T. Über die Zuordnung von Wellenfunktionen und Eigenwerten zu den Einzelnen Elektronen Eines Atoms. *Physica* **1934**, *1*, 104–113.
(47) Salzner, U.; Baer, R. Koopmans' Springs to Life. *J. Chem. Phys.* **2009**, *131*, 231101.
(48) Wasserman, H. H.; Floyd, M. B. The Oxidation of Heterocyclic Systems by Moleculr Oxygen—IV: The

Photosensitized Autoxidation of Oxazoles. *Tetrahedron* **1966**, *22*, 441–448.

(49) Wasserman, H. H.; Vinick, F. J.; Chang, Y. C. Reaction of Oxazoles with Singlet Oxygen. Mechanism of the Rearrangement of Triamides. *J. Am. Chem. Soc.* **1972**, *94*, 7180–7182.

(50) Marlier, J. F.; Dopke, N. C.; Johnstone, K. R.; Wirdzig, T. J. A Heavy-Atom Isotope Effect Study of the Hydrolysis of Formamide. *J. Am. Chem. Soc.* **1999**, *121*, 4356–4363.

(51) Csatayová, K.; Davies, S. G.; Fletcher, A. M.; Fowler, T. R.; Kennedy, M. S.; Roberts, P. M.; Thomson, J. E. Asymmetric Syntheses of 3-Deoxy-3-Aminosphingoid Bases: Approaches Based on Parallel Kinetic Resolution and Double Asymmetric Induction. *J. Org. Chem.* **2017**, *82*, 12447–12466.

(52) David, N.; Pasceri, R.; Kitson, R. R. A.; Pradal, A.; Moody, C. J. Formal Total Synthesis of Diazonamide A by Indole Oxidative Rearrangement. *Chem. – Eur. J.* **2016**, *22*, 10867–10876.

(53) Valdomir, G.; Fernández, M. de los Á.; Lagunes, I.; Padrón, J. I.; Martín, V. S.; Padrón, J. M.; Davyt, D. Oxa/Thiazole-Tetrahydropyran Triazole-Linked Hybrids with Selective Antiproliferative Activity against Human Tumour Cells. *New J. Chem.* **2018**, *42*, 13784–13789.

(54) Wang, Q.; Hou, X. H.; Wang, M. C. The Synthesis of Novel Chiral Ferrocenyl Aziridino Alcohol Ligands with Two Stereogenic Carbons and Structural Characteristics. *Adv. Mater. Res.* **2012**, *518–523*, 266–271.

(55) Inman, M.; Dexter, H. L.; Moody, C. J. Total Synthesis of the Cyclic Dodecapeptides Wewakazole and Wewakazole B. *Org. Lett.* **2017**, *19*, 3454–3457.

(56) Singh, S.; Prasad, N. R.; Kapoor, K.; Chufan, E. E.; Patel, B. A.; Ambudkar, S. V.; Talele, T. T. Design, Synthesis, and Biological Evaluation of (S)-Valine Thiazole-Derived Cyclic and Noncyclic Peptidomimetic Oligomers as Modulators of Human P-Glycoprotein (ABCB1). *ChemBioChem* **2014**, *15*, 157–169.

(57) Pietkiewicz, A. L.; Zhang, Y.; Rahimi, M. N.; Stramandinoli, M.; Teusner, M.; McAlpine, S. R. RITA Mimics: Synthesis and Mechanistic Evaluation of Asymmetric Linked Trithiazoles. *ACS Med. Chem. Lett.* **2017**, *8*, 401–406.

(58) White, G. A. Furan Carboxamide Fungicides: Structure-Activity Relationships with the Succinate Dehydrogenase Complex in Mitochondria from a Wild-Type Strain and a Carboxin-Resistant Mutant Strain of Ustilago Maydis. *Pestic. Biochem. Physiol.* **1988**, *31*, 129–145.

(59) Appiani, E.; Ossola, R.; E. Latch, D.; R. Erickson, P.; McNeill, K. Aqueous Singlet Oxygen Reaction Kinetics of Furfuryl Alcohol: Effect of Temperature, PH, and Salt Content. *Environ. Sci. Process. Impacts* **2017**, *19*, 507–516.

(60) Gaussian 09**,** Revision A.02, M. J. Frisch, G. W. Trucks, H. B. Schlegel, G. E. Scuseria, M. A. Robb, J. R. Cheeseman, G. Scalmani, V. Barone, G. A. Petersson, H. Nakatsuji, X. Li, M. Caricato, A. Marenich, J. Bloino, B. G. Janesko, R. Gomperts, B. Mennucci, H. P. Hratchian, J. V. Ortiz, A. F. Izmaylov, J. L. Sonnenberg, D. Williams-Young, F. Ding, F. Lipparini, F.. Egidi, J. Goings, B. Peng, A. Petrone, T. Henderson, D. Ranasinghe, V. G. Zakrzewski, J. Gao, N. Rega, G. Zheng, W. Liang, M. Hada, M. Ehara, K. Toyota, R. Fukuda, J. Hasegawa, M. Ishida, T. Nakajima, Y. Honda, O. Kitao, H. Nakai, T. Vreven, K. Throssell, J. A. Montgomery, Jr., J. E. Peralta, F. Ogliaro, M. Bearpark, J. J. Heyd, E. Brothers, K. N. Kudin, V. N. Staroverov, T. Keith, R. Kobayashi, J. Normand, K. Raghavachari, A. Rendell, J. C. Burant, S. S. Iyengar, J. Tomasi, M. Cossi, J. M. Millam, M. Klene, C. Adamo, R. Cammi, J. W. Ochterski, R. L. Martin, K. Morokuma, O. Farkas, J. B. Foresman, and D. J. Fox, Gaussian, Inc., Wallingford CT, 2016

(61) Ribeiro, R. F.; Marenich, A. V.; Cramer, C. J.; Truhlar, D. G. Use of Solution-Phase Vibrational Frequencies in Continuum Models for the Free Energy of Solvation. *J. Phys. Chem. B* **2011**, *115*, 14556–14562.